Synthetic community Hi-C benchmarking provides a baseline for virus-host inferences

Rokaiya Nurani Shatadru[1,2], Natalie E. Solonenko[1,2], Christine L. Sun[2], Matthew B. Sullivan[1,2,3,4,#]

5 [1] Department of Microbiology, The Ohio State University.

[2] Center of Microbiome Science, The Ohio State University.

[3] Byrd Polar and Climate Research Center, The Ohio State University.

[4] Department of Civil, Environmental and Geodetic Engineering, The Ohio State University.

[#] Corresponding author: sullivan.948@osu.edu; R914 Riffe Building, 496 W 12th Ave., Columbus,
10 OH 43210

Running title: **Hi-C performance in virus-host linkage inferences**

Keywords: Hi-C, Virus-Host Interactions, Genomics

Abstract

Microbiomes influence diverse ecosystems, but viruses increasingly appear to impose key constraints. While viromics has expanded genomic catalogs, host identification for these viruses remains challenging due to the limitations in scaling cultivation-based approaches and the uncertain reliability and relative low resolution of *in silico* predictions – particularly for understudied viral taxa. Towards this, Hi-C proximity ligation uses sequenced, cross-linked virus and host genomic fragments to infer virus-host linkages and has now been applied in at least nine studies. However, its accuracy remains unknown. Here we assess Hi-C performance in recovering virus-host interactions using synthetic communities (SynComs) composed of four bacterial strains and nine phages with known interactions and then apply optimized protocols to natural soil samples. In SynComs, standard Hi-C sample preparations and analyses showed poor normalized linkage score performance (26% specificity, 100% sensitivity, incorrect matches up to class level) that could be dramatically improved by Z-score filtering ($Z \geq 0.5$, 99% specificity), though at reduced sensitivity (62% down from 100%). Detection limits were established as reproducibility was poor below minimal phage abundances of 10^5 PFU/mL. Applying optimized protocols to natural soil samples, we compared Hi-C inferred virus-linkages with *in silico* bioinformatic predictions. Prior to Z-score thresholding, agreement was relatively high at the phylum to family levels (72%), but not at the genus (43%) or species (15%) levels. Z-score thresholding reduced sensitivity (only 34% of predictions were retained), with only modest improvements in congruence with bioinformatic methods (48% or 18% at genus or species levels, respectively). Regardless, this led to 79 genus-level-congruent virus-host linkages and 293 new ones revealed by Hi-C alone – i.e., providing many new virus-host interactions to explore in already well-studied climate-critical soils. Overall, these findings provide empirical benchmarks and methodological guidelines to improve the accuracy and reliability of Hi-C for virus-host linkage studies in complex microbial communities.

Introduction

Microbes drive many of the geochemical transformations that sustain Earth's systems (1) and are increasingly recognized for their critical roles in supporting plant (2) and animal (3) health – including humans where they can influence cravings, behavior, and susceptibility to disease (4). However, these microbial impacts are modulated by their ecosystem context where a complex network of interactions occur between microbes as they compete and/or partner (e.g., symbiosis) for niche space, acclimate to dynamic abiotic conditions, and/or combat predators. Towards the latter, viruses that infect microbes have emerged as prominent ecosystem components modulating microbial impacts – through infection that metabolically reprograms cells into 'virocells' that play vastly different roles to their uninfected counterparts, lysis that regulates near-term population dynamics, and gene flow that alters a population's longer-term evolutionary trajectories (5–8).

Problematically, while virus catalogs across diverse ecosystems are now exploding with tens to hundreds of thousands of large virus genome fragments routinely recovered per study [e.g., oceans (9–11) lakes (12), soils (6), and humans (13–15)], identifying hosts for these viruses remains challenging. For example, there are currently 15 million viruses with genomic representation at the centralized IMG/VR database, and only 7% of these have predicted virus-host relationships. Further, only a fraction (11%) of these have been experimentally validated (16). This is because cultivation-based approaches, while the gold standard for establishing 'infection', are both time consuming and limited to microbes that can be cultivated – often just a tiny fraction

of that observed in most ecosystems (16,17). As an alternative, experimental 'linkages' can be made using molecular PCR (18,19) or probe-based techniques that detect both virus and host markers simultaneously inside cells (20). However, these approaches do not scale to the community level as they rely upon database representation for primer/probe design, are time consuming to optimize, and target specific virus groups. Computational alternatives, i.e., bioinformatic methods to link viruses to hosts, are rapid and scale community-wide and so are most routinely used. However, novel viruses confound them (17) and even the most promising virus-host prediction tools that aggregate detection methods into a single prediction score (e.g., iPHoP (21) and VirMatcher (13)), remain largely untested experimentally.

Fortunately, a new method – proximity ligation sequencing via High-throughput Chromosome Conformation Capture (Hi-C) – offers scalable, experimental evidence for virus-host linkage, is broadly applicable, and has been implemented now across at least nine studies spanning diverse ecosystems (22–30). Conceptually, Hi-C captures DNA molecules that are physically proximate within a cell by cross-linking them using formaldehyde. Thus virus-host linkages could result from either active lytic virus infection or integrated prophages since viral genomes are close to host DNA. During Hi-C preparations such cross-linked DNA is then fragmentated with restriction enzymes and re-ligated to form a sequencing library, and subjected to high throughput sequencing (reviewed in (31)). The resulting reads are evaluated for virus-host chimeric reads, using either read recruitment or genome binning strategies. In the read recruitment approach, Hi-C reads are aligned to the reference virus and metagenome-assembled genomes (generally from the same sample), and linkages are inferred based on the frequency and pattern of chimeric reads connecting viral and host contigs (e.g. (22,24,26,27)). Alternatively, some studies used read alignments to reference genomes to generate a 'contact map', which is then used to bin genomes such that binned contigs are presumed to be proximal and if one is viral then it suggests a virus-host relationship (e.g. (23,30)).

Despite the growing use of Hi-C for identifying virus-host interactions, several challenges remain in interpreting these linkages. *First*, the associations inferred from Hi-C data have not been experimentally evaluated. To date, experimental validation using synthetic communities (SynComs) with known host linkages has not been done for virus-host linkages, but has been done for plasmid-host linkages (one study *Lactobacillus brevis* and its two plasmids) (32). *Second*, the Hi-C method remains largely unoptimized, as benchmarking efforts to assess sensitivity and specificity for virus-host relationships have been minimal. Of the nine published virus-host linkage studies, only one performed benchmarking and even then, it was limited to an *in silico* SynCom and relied solely on CRISPR spacer matches, without incorporating the many other computational features available for host prediction (30). *Finally*, computational analysis workflows for Hi-C analysis are not standardized with published studies employing diverse analytical approaches, thresholds, and cut-offs to infer linkages, which limits reproducibility and makes cross-study comparisons challenging. Together, these limitations highlight the need for systemic evaluation and methodological standardization to improve the reliability of Hi-C for virus-host linkage inference.

Here, we designed SynCom experiments with known virus-host interactions to assess Hi-C performance for linking viruses with their hosts. We used these experiments to develop analytic methods using the read recruitment approach to reduce spurious connections and improve virus-host identification accuracy. Additionally, we applied the resultant optimized Hi-C approaches to predict virus-host interactions in soil communities and compared these predictions to *in silico* methods to provide baseline comparative datasets and understanding for the field.

Materials and Methods

110 *Strains and growth conditions*

Four bacterial strains were used (**S1 Table**): *Cellulophaga baltica* strain 18 was isolated from the Baltic Sea in 2000 (hereafter CBA 18; (33)), while *Pseudoalteromonas* sp. H71, H105 and 13-15 were isolated from the North Sea in 1990 (hereafter PSA H71, PSA H105, and PSA 13-15; (34)). Nine bacteriophages were used: five infecting *C. baltica* strains and four infecting
115 *Pseudoalteromonas* strains (**S1 Table**). The CBA phages, φST, isolated on CBA 3 (strain not included in this study); φSM, isolated on CBA 3; φ46:1, isolated on CBA 46 (strain not included in this study); φ14:2, isolated on CBA 14 (strain not included in this study); and φ18:1, isolated on CBA 18, were isolated from the Baltic Sea between 2000 and 2005 (33). The PSA phages, PSA-HM1, isolated on PSA H71; PSA-HS4 isolated on PSA H105; PSA-HP1, isolated on PSA H100
120 (strain not included in this study); and PSA-HS2, isolated on PSA 13-15, were isolated from the North Sea in 1990 (35).

Bacteria were grown on Pseudoalteromonas-Cellulophaga (PC) plates (20.5g Sigma Sea Salts, 1.5g peptone, 1.5g proteose peptone, 0.6g yeast extract, 13g agar/L) at room temperature (RT). Single colonies were inoculated and grown stationary at RT overnight in PC liquid growth
125 medium (20.5g Sigma Sea Salts, 0.75g peptone, 0.5g yeast extract, 0.25g proteose peptone, 0.25g casamino acids, 1.5mL glycerol/L). Phage strains were stored in phage buffer (20.5g Sigma Sea Salts/L) and plaque forming units (PFUs) enumerated using the agar overlay method (36) with 3.5mL molten soft agar (20.5g Sigma Sea Salts and 6g low melting point agarose/L) and 300µl overnight bacterial culture per plate. Pairwise adsorption kinetics experiments were
130 conducted to determine the adsorption performance of each phage to each strain (**Supporting Information, S2 Table, S3 Table).**

Synthetic community sample collection

Three synthetic communities (SynCom-1, SynCom-2, and SynCom-3) were made, each
135 with three replicates. Accession numbers for all genomes used across SynComs are provided in **S1 Table**. All phage concentrations were based on infectious particles only, either when infecting bacterial hosts contained in the synthetic community or, for phages with no host in the synthetic community, on the host of isolation. Synthetic community 1 (SynCom-1) had equal numbers of each phage, whereas SynCom-2 and SynCom-3 had uneven numbers; final concentrations of
140 each bacterial strain and phage are given in **S1 Table**. Overnight cultures of each bacterial strain were transferred into fresh PC media and grown stationary at RT until mid-exponential phase and a concentration of $>1\times10^8$ colony forming units (CFU)/mL was reached. Concentration was determined by reading the optical density of each culture at 600 nm and using a regression equation of OD vs CFU/mL. A total of 5×10^8 CFUs from each mid-exponential bacterial strain
145 were combined in a 50 mL tube.

The nine phages were then added to each tube at the multiplicity of infection (MOI) indicated in **S1 Table**. After 15 minutes to allow phages to adsorb to their bacterial hosts, the community was diluted to 50 mL with PC phage buffer to slow adsorption and give a final cell concentration of 1×10^7 CFU/mL per strain. Aliquots of 1 mL were sampled, and flash frozen in
150 liquid nitrogen. Additional aliquots of each replicate for SynCom-1 were preserved prior to flash freezing with 6.5% v/v DMSO, 6% w/v betaine, or 20% v/v glycerol. Samples were stored at -80°C until processing. Cell recovery rates after freeze-thaw cycle were determined through CFU count and qPCR quantification of free DNA after freeze-thaw cycle (**Supporting Information, S4 Fig**).

155 *Peat sample collection and preparation*

In order to evaluate Hi-C performance in virus-host linkage from natural samples, we used three peat samples collected from a permafrost gradient in Stordalen Mire, Sweden. One sample was selected from each habitat: palsa, bog, fen, all collected in 2014. The samples were processed as described previously (37). Briefly, a soil core was collected from the surface (1-5
160 cm) for fen, bog, and palsa habitats, flash frozen in liquid nitrogen, and kept at -80°C until processing.

To establish a threshold based on known interactions, SynCom-1 was spiked into each peat sample at 1% of the total cell count. This concentration was chosen to minimize disruption of the native microbial community. The average cell count of the peat samples was 3.678×10^8
165 cells per gram soil, based on qPCR-based cell abundance data (38). Before Hi-C library preparation, 0.5 g of each peat sample was suspended in 2.5 mL nuclease-free water and vortexed for 5 min, pelleted at 500g for 5 min. An aliquot of SynCom-1 (62 µL, approximately 2×10^6 cells) was added to the supernatant to achieve a 1% spike-in.

170 *Hi-C sample library generation*

SynCom samples were thawed, and both these and the peat supernatants containing spike-ins were centrifuged to remove extracellular DNA. Resulting pellets were resuspended in the crosslinking solution provided in the ProxiMeta kit (Phase Genomics). Hi-C libraries were prepped from the resuspended solution for each replicate of the synthetic community or peat
175 sample, following the manufacturer's instructions. Samples were pooled and sequencing was performed by SeqCenter (Pittsburg, PA, USA) on an Illumina NovaSeq X 10B 300cyc lane, with the one exception of sample SynCom-1 replicate 1, which was sequenced at PhaseGenomics (Seattle, WA, USA) on an Illumina NovaSeq 6000. Raw sequencing files (fastq) of SynComs and peat samples are available in the NCBI Sequence Read Archive (PRJNA1252777 and
180 PRJNA1254298, respectively).

Unfortunately, for SynCom-1 preservative experiments, sequencing failed for one of the betaine-treated SynCom-1 replicates, and all glycerol-treated SynCom-1 samples. While successful samples yield over 100 million read pairs, these failed samples produced fewer than one million reads. The sequencing libraries from these samples had comparable yields to
185 successfully sequenced libraries, and the cause of failure remains unclear. Further, for SynCom-3, sequencing for replicate 3 failed, with few reads (under 5 million). Unlike the preservative treated samples above, these failed presumably due to low biomass in the prepared sequencing library. Because of the low sequencing output, these samples were excluded from further analysis.

190

Hi-C data processing (synthetic communities)

The read recruitment approach was selected for this study because the binning approach produces finalized bins that would exclude the negative controls present in the SynCom. Raw reads from each sample were quality-filtered using BBduk (BBmap suite) (39) to remove the
195 adapters and PhiX reads, and to trim and filter out low quality reads. BWA-MEM (40), with the -5SP flag, was used to align Hi-C reads from each sample to the reference genomes of SynCom members. Since the number of aligned reads depend on the length of the contig, number of restriction sites and the sequence coverage, normalization of raw linkage counts was performed. MetaCC (41), a binomial regression based normalization tool, was used with the enzyme flags
200 Sau3AI and MluCI (the restriction enzymes included in the Proximeta kit) to perform this

normalization. Subsequent analysis was conducted using the sparse matrix output 'Normalized_contact_matrix' from MetaCC. For genomes split across multiple contigs, contact scores were aggregated to produce a single normalized contact score for each virus-host pair. These normalized scores, along with associated Z-score (see below), are reported in **S6 Table**.

Z-scores were calculated for each SynCom replicate using the following equation:

$$Z = \frac{x - \mu}{\sigma}$$

where x is the contact score of a specific virus-host pair, μ is the mean contact score of all virus-host linkages in the sample, and σ is the standard deviation of those contact scores within the same sample.

Sensitivity and specificity of the predictions were calculated using the following equations:

$$Sensitivity = \frac{True\ Positives}{True\ Positives + False\ Negatives} \times 100$$

$$Specificity = \frac{True\ Negatives}{True\ Negatives + False\ Positives} \times 100$$

Hi-C data processing (peat samples)

To process the Hi-C metagenomic samples from peat, we utilized existing databases of metagenome-assembled genomes (MAGs) (42) and viral operational taxonomic units (vOTUs) (43,44) previously generated from the Stordalen Mire ecosystem. While it would have been possible to assemble MAGs and vOTUs directly from the specific peat samples analyzed, we opted to use datasets derived from multiple samples collected across the same region. This approach was intended to enhance comprehensiveness and improve the likelihood of detecting host–virus linkages. For the MAG dataset, the MAGs were clustered at 95% average nucleotide identity, resulting in a total of 2,073 non-redundant MAGs. In order to combine the two viral datasets, we used CheckV v0.8.1 (45) to cluster the vOTUs from each dataset at 95% nucleotide identity and minimum 80% coverage, yielding 5,828 total vOTUs. These were combined with host and viral genomes from the SynCom spike-in community to generate a comprehensive reference database for read recruitment.

Read recruitment and downstream processing using MetaCC followed the same protocol as applied to the SynCom samples. Normalized linkage scores and Z-scores for each genome are provided in **S9 Table**. It was common for individual viruses to be associated with multiple predicted hosts. This is not unexpected, as many viruses are known to infect more than one host species. However, to reduce complexity in downstream comparative analyses (see below), we retained only the top host prediction for each virus. Specifically, we included all normalized scores greater than zero to calculate Z-scores across potential virus–host linkages. For each virus, the host with the highest Z-score was selected as the primary linkage. Note that for viruses that were detected in multiple peat samples, we included them as separate instances.

Taxonomic comparisons

To ensure consistency in taxonomic predictions across different methods, we standardized our approach wherever possible. The Stordalen MAG V2 dataset was classified using GTDB-Tk

v2.3.2 (46) classify, with the r214 database and the option "--skip_ani_screen". For taxonomy determination via Hi-C linkage (i.e., vOTU to MAG connections), we applied the taxonomic annotations from the linked MAGs.

We used iPHoP v1.3.3 (21)) for virus-host prediction, conducting two separate: once with the default database ("Aug_2023_pub_rw")., and once with a custom database including the 95% ANI-clustered representative MAGs from the Stordalen Mire V2 dataset. For the default run, we executed the iphop predict command, using the default database without modification. For the custom database, we first processed the Stordalen Mire MAG representativeds with GTDB-tk, using the de_novo_wf workflow and recommended parameters. The resulting output was formatted into an iPHoP-compatible database using iphop add_to_db. Finally, we then ran iphop predict with this custom database. iPHoP produces two outputs: one that integrates predictions from both phage-based and host-based tools, and another that includes only host-based predictions. To obtain higher taxonomic resolution, we used the output incorporating host-based tools, which provides direct connections to MAGs capable of species-level classification. In contrast, the phage-based and host-based tools output typically yields genus-level predictions only (see iPHoP Bitbucket documentation for details). We combined the host-based results from both the default and custom runs. Since individual viruses can have multiple high-confidence hits (defined as confidence scores ≥90), we selected the top hit for each virus. In cases where multiple top hits had equivalent scores, one was chosen at random.

VirMatcher (version 0.4.29; (13)) was run with default parameters. Based on prior work, a confidence score of ≥3 was used as the threshold for high-confidence predictions. Compared to iPHoP, VirMatcher produced considerably fewer predictions for unique viruses (510 vs. 18, respectively). This discrepancy stems in part from the fact that many of the iPHoP linkages originated from public reference databases, while VirMatcher only utilized the Stordalen Mire MAGs. Due to the limited number of predictions generated by VirMatcher—particularly those overlapping with Hi-C linkages—we did not conduct further comparative analysis between VirMatcher and other tools.

Overlap between iPHoP and Hi-C predictions is presented in **S12 Table**, and the overlap between VirMatcher and Hi-C predictions is in **S13 Table**.

All scripts used for data preparation, analysis, and figure generation are available on GitHub: https://github.com/100dru/SynCom_Hi-C

Results and Discussion

1. Evaluating Hi-C performance using a SynCom

To evaluate the accuracy of Hi-C in identifying virus-host interactions, we designed an experiment using a SynCom composed of four well-characterized bacterial strains and nine phages (which are viruses that infect bacteria) with known relationships and infection efficiencies (12–14) (**Fig 1A, S1 Fig, S1 Table, S2 Table**). In this SynCom, *Cellulophaga baltica* strain 18 (CBA 18) has three infecting phages, and three *Pseudoalteromonas* strains (PSA 13-15, PSA H105, PSA H71) that could be infected by 2, 1, and 1 of these phage strains, respectively. Moreover, two additional *Cellulophaga baltica* phages that do not infect any strains were added to the SynCom as 'distractor' phages. This SynCom mix of bacteria and phage strains were chosen to examine how varying infection dynamics influenced Hi-C performance, including positive and negative interactions, and these quantitatively defined interactions were then used as the basis for Hi-C performance assessments.

Fig 1. Synthetic communities and experimental schema used to assess Hi-C virus-host linkages. **A.** Synthetic communities were built from four bacterial strains (CBA = *Cellulophaga baltica*; PSA = *Pseudoalteromonas*) and 9 phages (listed fully in **Table S1**) that were experimentally evaluated for infection in pairwise combinations via traditional plaque assays. Black boxes denote that the virus successfully plaques on the bacterial strain, whereas white (missing) boxes denote a negative, non-plaquing interaction. **B.** Schematic representation of the Hi-C experiment used to test virus-host relationships. After generating the synthetic community with the organisms mentioned above, Hi-C libraries were prepared and sequenced. Subsequently, bioinformatic analyses were performed to determine whether the expected virus-host linkages known from pairwise isolate-based experiments (denoted with black boxes) were observed.

To initially test Hi-C performance, we first constructed "SynCom-1", where bacteria and infective phage particles were added at high concentrations (10^7 CFU/mL for bacteria and 10^6 PFU/mL for phages) (**Fig 1A, S1 Table**). The multiplicity of infection (MOI) of 0.1, higher than common natural levels, was chosen to optimize Hi-C performance while minimizing multiply-infected bacteria. Phage amounts were adjusted based on infection efficiency (determined by plating) to ensure equal quantity of infectious phages across strains (**S1 Fig**). After combining the phages with bacteria, we incubated the mixture for 15 minutes to allow adequate phage adsorption, as pairwise experiments showed 74-99% adsorption within this time frame at MOI 0.1 (**S3 Table**). At the end of incubation, three technical replicates of SynCom-1 were immediately flash-frozen to halt phage activity (**Fig 1B**). Hi-C libraries were then prepared (PhaseGenomics ProxiMeta kit), and sequenced yielding 577 million 150-bp read pairs using standard Illumina sequencing approaches (see Materials and Methods).

SynCom-1 analyses revealed both expected and unexpected phage-host linkages. Expected linkages included all seven known interactions identified in prior single phage-host infection assays (**Fig 2, S1 Fig**), with 100% true positive detection (sensitivity) across three replicates (**S6 Table, S7 Table**). Unexpected linkages were for phage-bacteria pairs not known to infect that we included to represent negative interactions (**Fig 2, S1 Fig**). For example, φ14:2 lacked a corresponding host in SynCom-1, and yet it showed linkages with multiple bacterial strains, and this finding persisted even across replicates (**Fig 2B**). Quantitatively, we found that the rate of true negative predictions (specificity) was low under these initial conditions, with an average across replicates of only 26% (**S7 Table**). Replicate reproducibility was high with replicates 1 and 2 sharing thirty identical interactions as compared to replicate 2 missing only one interaction and replicate 3 missing only six interactions (**Fig 2B**).

Fig 2. Hi-C linkages from SynCom-1. A. Contact scores (left) and Z-scores (right) calculated for each replicate of SynCom-1, categorized by host strains. The black dots indicate correct virus-host linkages, the grey dots indicate incorrect virus-host linkages. The red vertical dotted line is drawn at Z-score = 0.5. **B.** Virus-host linkages determined from a non-zero normalized Hi-C score (left) or using a filtering approach (i.e., requiring a Z-score generated from non-score normalized HI-c scores above 0.5; right). The black boxes denote true positives, the grey boxes denote false positives, and the stripped boxes denote false negatives.

We next reasoned that the many false linkages might derive from the lack of a lower detection limit for the method, standard practice for new methods development for scientific disciplines at stage two (of four) or higher (47). To this end, we evaluated contact score magnitudes as a proxy for virus-host linkage prediction confidence and evaluated where specificity declined. Ideally, we expected similar contact scores for the same linkages across replicates within SynCom-1. However, variability was observed for both correct and incorrect linkages. For example, CBA 18 and φ18-1 (a known interaction) had contact scores of 170, 277, and 13 (normalized per 100,000 reads to account for sequencing depth differences) in replicates 1, 2, and 3, respectively. Similarly, CBA 18 and HM1 (which do not have a known interaction), had contact scores of 41, 179, and 6 (normalized per 100,000 reads). Despite these variations, we observed that correct linkages generally had higher contact scores than incorrect ones (**Fig 2A,** black vs grey dots) such that 85% of the time, the highest contact score for each phage was to its correct host **(S2 Fig).** Nevertheless, contact score variability presents a challenge for establishing a universal threshold to minimize false positives solely from this metric.

Given this, we evaluated contact score performance in context with receiver operating characteristics (ROC) curves (42) to assess whether such models might improve the ability to distinguish between correct and incorrect linkages across replicates. Applying such approaches to SynCom-1 data resulted in an ROC curve with an area under the curve (AUC) of 0.71. This suggested that the contact scores can differentiate linkages (with AUC values closer to 1 representing better performance), but also that there was some room to improve upon the false positive rate (**S3 Fig**). While other studies had mitigated such noise via applying cut-offs for inter-genome and intra-genome ratios (e.g., a ratio of 0.6) or requiring a minimum number of linkages (e.g., 2 or 10 linkages), no statistical evaluations of effectiveness were conducted (see literature overview in **S8 Table**).

To remedy this, we posited that Z-scores might be useful due to their value in RNA-Seq analyses for identifying differentially expressed genes (43) via considering each point relative to the mean. Indeed, converting SynCom-1 contact scores to Z-scores revealed that most correct and incorrect linkages had Z-scores above or below 0, respectively (**Fig 2A**), and the ROC curve improved the AUC to 0.93 (**S3 Fig**). The increased AUC (0.71 for contact scores to 0.93 for Z-scores) suggested that Z-scores more correctly identify virus-host linkages. Looking at the ROC curve further (**S3 Fig**), we selected a conversative threshold of 0.5 since it yielded the highest specificity and sensitivity across replicates. At this conservative threshold, 83% of virus-host linkages were removed with an impact of reducing average sensitivity across the replicates from 100% to 62%, while drastically increasing the average specificity from 26% to 99% (**S7 Table**). Further, this Z-score-based threshold showed consistent performance across all replicates. While this is promising, we caution that further evaluation across future sample types and datasets will be valuable for assessing its universality, particularly for the specific Z-score cut-off used.

2. *Assessing Hi-C performance under different sample preservation conditions*

With analytical optimization suggesting promise for Hi-C-based virus-host linkage approach, we recognized that vast archives of already-preserved samples might be an enticing

opportunity to be repurposed towards this approach. Given this, we evaluated sample preservation conditions to help guide researchers on best practices. Also, anecdotal observations from our own work had suggested nuances of preservation might be important as in the above experiments where we freeze-thawed the samples before Hi-C library preparation, we observed unexpected SynCom-1 linkages even after the analytical optimizations. For example, the correct linkages for PSA 13-15 (to HS2), PSA H105 (to HS4) and CBA 18 (to φST) had Z-scores under the threshold (Z scores < 0.5) (**Fig 2**). While the reduced linkage scores for φST can be attributed to its slow adsorption (i.e., not detectable within 15 min), the other phages exhibit faster adsorption (**S2 Table**) and so we expected to detect their linkages and yet did not.

Assuming possible freeze-thaw effects during sample preparation that impact linkage inferences, we hypothesized differentially affected recovery of intact versus leaky cells that could reduce true linkages and increase non-specific linkages detected. To test this, we performed a freeze-thaw experiment to assess recovery of viable cells and DNA leakage. This revealed that PSA 13-15, PSA H105 and PSA H71 CFUs recovered poorly from freeze-thaw (1% on average, ranging from 0.1 - 1.8%), whereas CBA 18 had approximately 100% recovery (**Supplementary Information, S4A Fig**). Additionally, free DNA recovered from post-freeze thaw samples was 14- to 17-fold higher than pre-freeze in unpreserved PSA strains, while that from CBA18 did not increase (**S4B Fig**). Together these findings suggest that PSA strains were more prone to leakage following freeze-thaw and suggest more broadly that host cellular integrity following freeze-thaw will variably impact Hi-C linkage performance in natural communities.

To assess whether cryoprotective agents could improve Hi-C performance by increasing cell viability and reducing leakiness, we evaluated commonly used cryoprotectants. Cryoprotective agents, such as dimethyl sulfoxide (DMSO) and glycerol, protect cells from cryoinjuries by inhibiting water crystallization while betaine prevents osmotic rupture during the freeze-thaw cycle . We first assessed whether treating with DMSO, glycerol, or betaine, could improve cell viability and reduce leakiness prior to Hi-C library preparation and sequencing. Indeed, all three cryoprotective agents increased cell recovery (to 20% on average, 1-60% range) for PSA 13-15, PSA H105 and PSA H71 (**S4A Fig**) and reduced cell leakiness (to 3.5-fold more free DNA than pre-freeze on average, 1.6 to 4.4-fold range) (**S4B Fig**). These results suggest that the cryoprotective agents improved cell viability in isolation, which may, in turn, enhance Hi-C performance in virus-host linkage.

Given this, we assessed SynCom-1 Hi-C performance using samples that were flash frozen compared to those preserved with DMSO, betaine, and glycerol (**Fig 3**). Only DMSO (3 replicates) and betaine (2 replicates) could successfully be Hi-C library prepared, while none of the 3 glycerol replicates were successful (see Materials and Methods). For those replicates that led to sequencing libraries and data, we examined the specific linkages between PSA 13-15 (to HS2), PSA H105 (to HS4), and CBA 18 (to φST) in the cryopreserved samples to determine if they improved. Despite having similar total linkages **(S5 Table)**, there was no consistent improvement in the cryopreserved samples for these linkages. The only (slight) improvement being DMSO-treated SynCom-1 samples where PSA H105 - HS4 linkages were detected above Z-score threshold in two out of three replicates. Together these data suggest that tested cryoprotective agents tested do not drastically improve cryo-sensitive virus-host linkages, possibly due to their interference with Hi-C sequencing library preparation. While not evaluated directly here, we posit that chemical interactions between cryoprotective agents and Hi-C library preparation reagents may impact sample processing outputs.

Fig 3. Cryopreservation experiment to assess impact on SynCom-1 Hi-C linkages. A. All Z-scores (left) and virus-host linkages (right) for each replicate of SynCom-1 cryopreserved with DMSO and categorized by host strains. Black and gray dots indicate correct or incorrect virus-

host linkages, respectively, while black, gray, and striped boxes indicate true and false positives, and false negatives, respectively. The red vertical dotted line is drawn at Z-score = 0.5. **B.** Same data type as A, but for betaine-preserved samples. **C.** Average sensitivity (gray bar) and specificity (black bar) rates calculated for SynCom-1 treated with and without cryoprotective agents.

Beyond specific linkages, we also examined whether there were major differences in overall linkages between the flash-frozen and cryoprotected samples to guide researchers on whether already-preserved archived samples might now be re-purposed for making virus-host predictions. Starting with raw linkages, we observed similar levels of non-self linkages across sample types (14% for betaine, 11% for DMSO, versus 11% for flash-frozen) (**S5 Table**). After filtering for Z-scores ($Z \geq 0.5$), DMSO- and betaine-treated samples showed similar specificity to the flash frozen sample (96%, 97%, and 99% on average, respectively). However, sensitivity was generally lower in cryoprotective-treated SynCom-1 compared to flash-frozen samples. The betaine-treated samples showed clearer results (43% across all replicates), while the DMSO-treated samples had less consistent results (57%, ranging from 29% to 86%). In contrast, the flash-frozen samples had more consistent results (62%, ranging from 57% to 71%). (**Fig 3C)**. These data suggest that flash-frozen samples performed the best overall, as cryoprotectants might reduce sensitivity, but that DMSO- and betaine-treated samples do have value for later Hi-C analysis if those are the only sample options available.

3. Evaluating the detection limit of Hi-C performance

Given analytical and cryopreservation promise, we next sought to assess detection limits for Hi-C virus-host linkage inferences by examining flash-frozen SynComs with varying virus and host concentrations. This is because SynCom-1 concentrations where all phages were at 10^6 PFU/mL with host-relevant MOIs of 0.1 (**S1 Table**), and such concentrations are relatively high for natural samples. To better reflect natural conditions, we created two new SynComs – SynCom-2 and SynCom-3 – where phage concentrations ranged from 10^3 – 10^6 PFU/mL and MOIs ranged between 0.0001 to 0.1 as host concentrations were held constant at 10^7 PFU/mL for each bacterial strain (**S1 Table**). Three technical replicates of SynCom-2 and SynCom-3 were attempted to assess reproducibility, though one replicate of SynCom-3 failed Hi-C proximity ligation sequencing post library preparation. Presumably, this was due to low biomass since this was the lowest concentration tested with DNA concentrations (0.070 ng/μL) near the lower threshold required for successful library generation according to the guidelines for the PhaseGenomics ProxiMeta kit.

From the five remaining successful Hi-C proximity ligation libraries, their resultant sequence data revealed clear detection limits. On the one hand, these libraries were comparable to those from SynCom-1 as an average of 14% and 13% of linkages were non-self in SynCom-2 and SynCom-3, respectively, which was only slightly higher than SynCom-1 (11%). On the other hand, problematically, Z-score threshold analyses ($Z \geq 0.5$) revealed that only one linkage passed the threshold in these latter SynComs across all the replicates (**Fig 4**). This one linkage was phage φ18:1 in SynCom-2 and phage φ46:1 in SynCom-3, and in both cases these phages were the only ones added at high concentrations of 10^6 PFU/mL (MOI = 0.1). Other phages added at 10^5 PFU/mL (MOI = 0.01) – φST in SynCom-2 and HS4 in SynCom-3 – had observable linkage data, but at Z-scores below the threshold ($Z < 0.5$) such that they were indistinguishable from incorrect linkages. Given that only the phages at 10^6 PFU/mL phages had a detected linkage, there was an average of 100% specificity for both, but because of the absence of linkages for the other phages present in the SynComs, only 15% and 14% sensitivity was observed across SynCom-2 and SynCom-3, respectively.

Fig 4. Detection limit experiment to evaluate Hi-C linkages in varied concentration SynCom-2 and SynCom-3. A. All Z-scores (left) and virus-host linkages (right) for each replicate of SynCom-2**,** categorized by host strains. All figure elements are the same as described in **Fig 3**. **B.** Same data type as A, but for SynCom-3. **C.** Average sensitivity and specificity rates calculated for SynCom-1, SynCom-2, and SynCom-3 without cryoprotective agents. The grey bar represents sensitivity, and the black bar represents specificity.

Such a high minimum concentration required for accurate Z-score-based thresholding suggests that Hi-C-based virus-host linkages will be limited to the more abundant taxa in natural samples and that researchers should consider 10^6 PFU/mL a tentative lower detection limit. This rather high detection limit invites future methods optimization work if Hi-C-based virus-host linkage approaches are to have value across a diversity of samples in future work.

4. Evaluating Hi-C linkages in natural communities

With analytical, cryopreservation, and detection limits now better understood, we sought to evaluate SynCom-derived Z-score thresholding approaches in natural communities. Specifically, we applied Hi-C analysis to flash-frozen permafrost thaw gradient samples collected from the well-studied, climate-critical model ecosystem, Stordalen Mire, in northern Sweden (38,49–51). We selected three flash-frozen peat samples from surface layer soils of the dominant permafrost thaw stages at this site: palsa, bog, and fen (from least to most thawed). In response to recent recommendations for using spike-ins to enhance post-sequencing quantitative inferences (52–55), we then spiked these samples with ~2×10^6 cells of SynCom-1 into each 0.5 g peat sample prior to Hi-C library generation. We estimated that this would represent approximately 1% of the total cells in these samples (37) (see Materials and Methods) and as such could provide thresholding data for true and false linkage inferences for later interpretation.

We analyzed the resulting Hi-C peat sequencing datasets to identify virus-host linkages using the same method as applied to the SynComs. Briefly, we performed read recruitment to the spike-in genomes and a comprehensive dataset of *de novo* microbial and viral genomes including 2,074 metagenome-assembled-genomes (MAGs) (42) and 5,828 virus-operational-taxonomic-units (vOTUs) generated from Stordalen Mire peat samples (43,44). To address the microbial complexity inherent in soil samples, we performed deep sequencing to maximize linkage detection, applying 453M, 528M, and 326M total reads for palsa, bog, and fen samples, respectively. On average, 80% of the reads recruited to our reference genomes, with 0.001% (6,064) being chimeric virus-host sequencing reads deemed suitable for further evaluation. Unfortunately, despite the substantial sequencing, the spike-in experiment yielded few virus-host linkages from SynCom-1. Specifically, only two correct pairs (CBA 18 linked to φ18:1 and φ46:1) detected in the bog sample, and one incorrect pair (a peat MAG to 14:2) in the fen sample, and all these pairs had low Z-scores (< 0.5). These findings demonstrate that while spike-ins are ideal for quantitative work (52–55), optimizing spike-in inocula for field samples, particularity in soils, presents numerous challenges. However, these data remained informative as follows.

First, comparison of normalized Hi-C linkage patterns across synthetic and natural peat communities revealed broadly similar proportions of virus-host associations, despite notable variation in linkage abundance and taxonomic predictions among habitats. Hi-C linkage patterns revealed similar proportions of virus-host linkages across peat samples and SynCom-1 (**S5 Fig**), indicating consistent linkage behavior between synthetic and natural communities. However, the number of virus-host linkages varied substantially by habitat bog the highest with 5,729 virus-host linkages (1 per 100,000 reads), followed by fen with 677 (0.2 per 100,000 reads), then palsa with 108 (0.02 per 100,000 reads) (**S5 Fig**). Such variation may reflect technical differences or

underlying biological variation, such as differences in active viral infections (or prophage) activity across samples, known to vary in Stordalen Mire (44). Of 6,064 virus-host linkages identified across peat samples, most vOTUs were linked to multiple contigs within or across MAGs. To reduce redundancy and spurious associations, only the highest normalized contact score per virus was retained, resulting in 495 unique virus-host associations spanning 19 microbial phyla (**S9 Table**). These linkages involved 30, 373, and 110 individual vOTUs from the palsa, bog, and fen habitats, respectively. Acidobacteria were the most frequently predicted host phylum (95 viruses), consistent with their prevalence in Stordalen Mire (38). Host taxonomic profiles varied by habitat, likely reflecting habitat-specific differences in microbial community composition (38). For example, while many phyla were shared among multiple habitats, Bacteroidota hosts were more predominant in the fen as evidenced by existing literature (**S6 Fig**). Although all 495 associations would be considered valid based on alignment-based Hi-C classification methods, further validation is needed to confirm their biological relevance.

Second, given the Hi-C-based virus-host linkages, we next aimed to assess how these associations compared to *in silico* host predictions to evaluate congruence. For *in silico* predictions, we used two tools that aggregate host predictions made from multiple approaches either via machine learning as in iPHoP (21) or a literature-derived importance valuation incorporated into a probabilistic model as in VirMatcher (13). Our goal was to assess congruence at the species level where possible, to capture the most ecologically relevant taxonomic resolution. VirMatcher provides linkages from vOTUs to a user submitted database (in this case, the Stordalen Mire MAGs), whereas for iPHoP we used host-based predictions only, which links vOTUs and a combined large public database alongside our custom-addition of Stordalen Mire MAGs (see Materials and Methods). Of the 5,828 Stordalen Mire vOTUs analyzed, iPHoP and VirMatcher were able to make confident host predictions for 1,640 vOTUs (score ≥ 90) and 412 vOTUs (final score ≥ 3), respectively (**S10 Table, S11 Table**). Of these, 12% (200 vOTUs) for iPHoP and 4% (16 vOTUs) for VirMatcher also had a corresponding Hi-C linkage (**Fig 5A, S12 Table, S13 Table**). An additional 293 vOTUs were linked to hosts exclusively through Hi-C data (**Fig 5A**). However, when considering all normalized Hi-C contact scores, congruence between overlapping predictions was low. Only 43% (92 viruses) of iPHoP predictions and 67% (12 viruses) of VirMatcher predictions were congruent with Hi-C data at the genus level. Given that these predictions were supported across independent lines of evidence, we considered these congruent predictions to be higher-confidence virus-host linkages.

Fig 5. Comparison of virus-host prediction from Hi-C and *in silico* tools. A. Venn diagrams showing the overlap of viruses with host predictions among Hi-C, iPHoP and VirMatcher. The left panel includes all viruses with predictions, while the right panel includes only Hi-C predictions with a Z-score ≥ 0.5. **B.** Comparison of virus-host predictions across all samples between Hi-C and iPHoP, shown with and without applying a Z-score filter for the Hi-C linkages. Black bars indicate congruent predictions identified from both tools and grey bars indicate non-congruent predictions. Note: Although many viruses had multiple predicted hosts from each tool, only the top-scoring prediction for each virus was considered in this comparison.

Third, to further understand congruence between methods, we focused on the iPHoP and Hi-C predictions, since there were more data available for analyses, and assessed congruence across taxonomic levels (**Fig 5B**). Without applying any filtering on the Hi-C linkages, congruence at the domain level was nearly complete (99%) but declined at finer taxonomic ranks, with phylum to family levels showing approximately 72% congruency and genus and species levels showing 43% and 15% (excluding the 155 predictions lacking a species assignment) congruence, respectively (**S7 Fig)**. Z-score thresholding, i.e., applying a confidence threshold of Z ≥ 0.5 to the Hi-C predictions, reduced the number of overlapping predictions from 214 to 142 and modestly improved congruency across most taxonomic levels – domain: 99%, phylum-class: 83%, genus:

48%, species: 18% (excluding the 104 predictions lacking a species assignment) (**S8 Fig**). These results suggest that while high-confidence computational predictions are largely consistent with Hi-C associations at broader taxonomic levels, they diverge at finer scales, particularly at the genus and species levels. The latter is critical given such higher taxonomic ranks are where ecological relevance becomes more pronounced. When considering matches excluded through Z-score filtering, we observed a decline in congruent assignments (potentially spurious) and an increase in incongruent ones (potentially authentic) with increasing taxonomic resolution. For instance, at the phylum level, filtering removed 49 congruent and 23 incongruent matches, whereas at the genus level, 29 congruent and 49 incongruent matches were excluded (**S8 Fig**). Although interpretation remains challenging, we assume that higher concordance between methods represents an increased likelihood of accuracy.

Due to differences in experimental and bioinformatic methodologies across published studies that infer virus-host linkages using the Hi-C approach, direct comparisons of our Hi-C results to the literature are challenging. This is because robust comparisons would require reanalyzing all published datasets in a systematic manner, which was impossible due to key underlying data of various types missing from most studies. However, a recent study (26) employed a similar approach as the one used in our study (using read recruitment to infer linkages and normalizing these linkages with binomial regression analysis) and provided the data in an analysis friendly format. Using the published virus-host linkage (Supplementary Table 10 from (26)), we calculated Z-scores and applied our filtering based on highest linkages for each viral metagenome assembled genome (vMAG) (**S14 Table).** This revealed that only 30% (14 out of 47) of their reported vMAGs had predictions that exceeded the Z-score threshold ($Z \geq 0.5$). Notably, this removed cross-domain and cross-phyla interaction predictions. While a $Z \geq 0.5$ threshold may not be universally appropriate, our SynCom data indicate that it effectively removes spurious linkages. For other natural systems, it may be beneficial to assess congruency with *in silico* bioinformatic tools to strike an appropriate balance between sensitivity and specificity—choosing which predictions to prioritize, at which taxonomic levels, and with what tolerance for potential false positives.

Conclusion

Identifying hosts for viruses is crucial for advancing our understanding of viral ecology and the complex interactions within microbiomes that shape ecosystems worldwide. In this study, we optimized analytical approaches for using Hi-C proximity ligation to identify virus-host linkages and benchmarked this method for sensitivity, accuracy, detection limits, and sample preservation using synthetic communities (SynComs) with known interactions. Our findings demonstrate that applying a Z-score threshold significantly improves the accuracy and sensitivity of virus-host linkage detection via Hi-C, albeit with a reduction in the number of predicted associations. By increasing specificity, our approach enhances confidence in host predictions and provides a more reliable framework for studying viruses in complex ecosystems. However, this comes with the inherent trade-off between sensitivity and specificity. Fewer host predictions are made, but with greater robustness. Future research will benefit analytically from providing all relevant data needed for re-analyses, as well as community consensus towards standardized analytical approaches that incorporate more advanced bioinformatics to protect against false positives. On the experimental side, future methods development is needed to reduce spurious cross-linking through refined fixation protocols, optimized experimental conditions, or improved sample preservation – ideally to reduce the detection limit to much lower than the current 10^5 PFU/ml identified in this study. Ultimately, refining Hi-C methods will be a critical step towards more accurately capturing virus-host interactions and mechanistically integrating viral dynamics into

ecological models at various scales. These advancements have the potential not only to deepen our understanding of viral roles in ecosystems but also to inform practical applications such as phage therapeutics and the design of targeted phage cocktails, with broad implications across environmental and medical research.

Competing Interests

None

Acknowledgments

We thank the EMERGE field team and Dr. Fen Li for the collection and the management of the soil samples. We thank Dr. Ben Bolduc, Dr. Garrett Smith and James Riddell for bioinformatic assistance, Dr. Yuxuan Du for MetaCC troubleshooting assistance and discussions, Dr. Olivier Zablocki and Dr. Suzanne Hodgkins for manuscript preparation assistance and data management assistance. We also thank Dr. Karna Gowda for his valuable advice on statistical inferences. Discussions at the Ohio State International Viromics Workshop (2024) were also helpful for working through literature nuances and anecdotes. This work was supported by (sub) awards to MBS from the U.S. Department of Energy, Office of Science, Office of Biological and Environmental Research, under Award Number DE-SC0023307, the National Science Foundation, Biology Integration Institutes Program, Award #2022070, and the National Institutes of Health, R01AI169865.

References

1. Falkowski PG, Fenchel T, Delong EF. The microbial engines that drive Earth's biogeochemical cycles. Science. 2008 May 23;320(5879):1034–9.

2. Trivedi P, Leach JE, Tringe SG, Sa T, Singh BK. Plant–microbiome interactions: from community assembly to plant health. Nat Rev Microbiol. 2020 Nov;18(11):607–21.

3. Levin D, Raab N, Pinto Y, Rothschild D, Zanir G, Godneva A, et al. Diversity and functional landscapes in the microbiota of animals in the wild. Science. 2021 Mar 25;372(6539):eabb5352.

4. Fan Y, Pedersen O. Gut microbiota in human metabolic health and disease. Nat Rev Microbiol. 2021 Jan;19(1):55–71.

5. Brum JR, Sullivan MB. Rising to the challenge: accelerated pace of discovery transforms marine virology. Nat Rev Microbiol. 2015 Mar;13(3):147–59.

6. Graham EB, Camargo AP, Wu R, Neches RY, Nolan M, Paez-Espino D, et al. A global atlas of soil viruses reveals unexplored biodiversity and potential biogeochemical impacts. Nat Microbiol. 2024 Jul;9(7):1873–83.

7. Tobin CA, Hill C, Shkoporov AN. Factors Affecting Variation of the Human Gut Phageome. Annu Rev Microbiol. 2023 Sep 15;77(Volume 77, 2023):363–79.

8. Howard-Varona C, Lindback MM, Fudyma JD, Krongauz A, Solonenko NE, Zayed AA, et al. Environment-specific virocell metabolic reprogramming. ISME J. 2024 Jan 1;18(1):wrae055.

9. Roux S, Brum JR, Dutilh BE, Sunagawa S, Duhaime MB, Loy A, et al. Ecogenomics and potential biogeochemical impacts of globally abundant ocean viruses. Nature. 2016 Sep;537(7622):689–93.

10. Gregory AC, Zayed AA, Conceição-Neto N, Temperton B, Bolduc B, Alberti A, et al. Marine DNA Viral Macro- and Microdiversity from Pole to Pole. Cell. 2019 May;177(5):1109-1123.e14.

11. Dominguez-Huerta G, Zayed AA, Wainaina JM, Guo J, Tian F, Pratama AA, et al. Diversity and ecological footprint of Global Ocean RNA viruses. Science. 2022 Jun 10;376(6598):1202–8.

12. Zhou Z, Tran PQ, Martin C, Rohwer RR, Baker BJ, McMahon KD, et al. Unravelling viral ecology and evolution over 20 years in a freshwater lake. Nat Microbiol. 2025 Jan;10(1):231–45.

13. Gregory AC, Zablocki O, Zayed AA, Howell A, Bolduc B, Sullivan MB. The Gut Virome Database Reveals Age-Dependent Patterns of Virome Diversity in the Human Gut. Cell Host Microbe. 2020 Nov 11;28(5):724-740.e8.

14. Camarillo-Guerrero LF, Almeida A, Rangel-Pineros G, Finn RD, Lawley TD. Massive expansion of human gut bacteriophage diversity. Cell. 2021 Feb 18;184(4):1098-1109.e9.

15. Shkoporov AN, Clooney AG, Sutton TDS, Ryan FJ, Daly KM, Nolan JA, et al. The Human Gut Virome Is Highly Diverse, Stable, and Individual Specific. Cell Host Microbe. 2019 Oct 9;26(4):527-541.e5.

16. Camargo AP, Nayfach S, Chen IMA, Palaniappan K, Ratner A, Chu K, et al. IMG/VR v4: an expanded database of uncultivated virus genomes within a framework of extensive functional, taxonomic, and ecological metadata. Nucleic Acids Res. 2023 Jan 6;51(D1):D733–43.

17. Edwards RA, McNair K, Faust K, Raes J, Dutilh BE. Computational approaches to predict bacteriophage–host relationships. Smith M, editor. FEMS Microbiol Rev. 2016 Mar;40(2):258–72.

18. Tadmor AD, Ottesen EA, Leadbetter JR, Phillips R. Probing individual environmental bacteria for viruses by using microfluidic digital PCR. Science. 2011 Jul 1;333(6038):58–62.

19. Sakowski EG, Arora-Williams K, Tian F, Zayed AA, Zablocki O, Sullivan MB, et al. Interaction dynamics and virus–host range for estuarine actinophages captured by epicPCR. Nat Microbiol. 2021 May;6(5):630–42.

20. Barrero-Canosa J, Moraru C. PhageFISH for Monitoring Phage Infections at Single Cell Level. Methods Mol Biol Clifton NJ. 2019;1898:1–26.

21. Roux S, Camargo AP, Coutinho FH, Dabdoub SM, Dutilh BE, Nayfach S, et al. iPHoP: An integrated machine learning framework to maximize host prediction for metagenome-derived viruses of archaea and bacteria. PLOS Biol. 2023 Apr 21;21(4):e3002083.

22. Bickhart DM, Watson M, Koren S, Panke-Buisse K, Cersosimo LM, Press MO, et al. Assignment of virus and antimicrobial resistance genes to microbial hosts in a complex microbial community by combined long-read assembly and proximity ligation. Genome Biol. 2019 Aug 2;20(1):153.

23. Marbouty M, Thierry A, Millot GA, Koszul R. MetaHiC phage-bacteria infection network reveals active cycling phages of the healthy human gut. Duerkop BA, Garrett WS, Duerkop BA, Quince C, editors. eLife. 2021 Feb 26;10:e60608.

24. Ivanova V, Chernevskaya E, Vasiluev P, Ivanov A, Tolstoganov I, Shafranskaya D, et al. Hi-C Metagenomics in the ICU: Exploring Clinically Relevant Features of Gut Microbiome in Chronically Critically Ill Patients. Front Microbiol. 2021;12:770323.

25. Cuscó A, Pérez D, Viñes J, Fàbregas N, Francino O. Novel canine high-quality metagenome-assembled genomes, prophages and host-associated plasmids provided by long-read metagenomics together with Hi-C proximity ligation. Microb Genomics. 2022 Mar 17;8(3):000802.

26. Hwang Y, Roux S, Coclet C, Krause SJE, Girguis PR. Viruses interact with hosts that span distantly related microbial domains in dense hydrothermal mats. Nat Microbiol. 2023 Apr 6;1–12.

27. Cheng Z, Li X, Palomo A, Yang Q, Han L, Wu Z, et al. Virus impacted community adaptation in oligotrophic groundwater environment revealed by Hi-C coupled metagenomic and viromic study. J Hazard Mater. 2023 Sep 15;458:131944.

28. Wu R, Davison MR, Nelson WC, Smith ML, Lipton MS, Jansson JK, et al. Hi-C metagenome sequencing reveals soil phage–host interactions. Nat Commun. 2023 Nov 23;14(1):7666.

29. Marbouty M, Baudry L, Cournac A, Koszul R. Scaffolding bacterial genomes and probing host-virus interactions in gut microbiome by proximity ligation (chromosome capture) assay. Sci Adv. 2017 Feb 17;3(2):e1602105.

30. Du Y, Fuhrman JA, Sun F. ViralCC retrieves complete viral genomes and virus-host pairs from metagenomic Hi-C data. Nat Commun. 2023 Jan 31;14(1):502.

31. Lajoie BR, Dekker J, Kaplan N. The Hitchhiker's Guide to Hi-C Analysis: Practical guidelines. Methods San Diego Calif. 2015 Jan;72:65–75.

32. Beitel CW, Froenicke L, Lang JM, Korf IF, Michelmore RW, Eisen JA, et al. Strain- and plasmid-level deconvolution of a synthetic metagenome by sequencing proximity ligation products. PeerJ. 2014 May 27;2:e415.

33. Holmfeldt K, Middelboe M, Nybroe O, Riemann L. Large Variabilities in Host Strain Susceptibility and Phage Host Range Govern Interactions between Lytic Marine Phages and Their Flavobacterium Hosts. Appl Environ Microbiol. 2007 Nov;73(21):6730–9.

34. Wichels A, Biel SS, Gelderblom HR, Brinkhoff T, Muyzer G, Schütt C. Bacteriophage diversity in the North Sea. Appl Environ Microbiol. 1998 Nov;64(11):4128–33.

35. Duhaime MB, Wichels A, Sullivan MB. Six Pseudoalteromonas Strains Isolated from Surface Waters of Kabeltonne, Offshore Helgoland, North Sea. Genome Announc. 2016 Feb 11;4(1):e01697-15.

36. Sambrook J. Molecular Cloning: A Laboratory Manual. Cold Spring Harbor Laboratory; 2003. book.

37. Wilson RM, Zayed AA, Crossen KB, Woodcroft B, Tfaily MM, Emerson J, et al. Functional capacities of microbial communities to carry out large scale geochemical processes are maintained during ex situ anaerobic incubation. PLOS ONE. 2021 Feb 25;16(2):e0245857.

38. Woodcroft BJ, Singleton CM, Boyd JA, Evans PN, Emerson JB, Zayed AAF, et al. Genome-centric view of carbon processing in thawing permafrost. Nature. 2018 Aug;560(7716):49–54.

39. BBMerge – Accurate paired shotgun read merging via overlap | PLOS ONE [Internet]. [cited 2023 Jul 12]. Available from: https://journals.plos.org/plosone/article?id=10.1371/journal.pone.0185056

40. Li H, Durbin R. Fast and accurate short read alignment with Burrows-Wheeler transform. Bioinforma Oxf Engl. 2009 Jul 15;25(14):1754–60.

41. Du Y, Sun F. MetaCC allows scalable and integrative analyses of both long-read and short-read metagenomic Hi-C data. Nat Commun. 2023 Oct 6;14(1):6231.

42. Guo J, Aroney S, Dominguez-Huerta G, Smith D, Vik D, Ansah CO, et al. Mobile genetic elements that shape microbial diversity and functions in thawing permafrost soils [Internet]. Microbiology; 2025 [cited 2025 Mar 7]. Available from: https://www.biorxiv.org/content/10.1101/2025.02.12.637893v2.abstract

43. Emerson JB, Roux S, Brum JR, Bolduc B, Woodcroft BJ, Jang HB, et al. Host-linked soil viral ecology along a permafrost thaw gradient. Nat Microbiol. 2018 Aug;3(8):870–80.

44. Sun CL, Pratama AA, Gazitúa MC, Cronin D, McGivern BB, Wainaina JM, et al. Virus ecology and 7-year temporal dynamics across a permafrost thaw gradient. Environ Microbiol. 2024 Jul;26(8):e16665.

Supporting Information

Supporting Information

S1 Fig. Efficiency of plating for members of the SynCom-1 community. Here, the infectivity is derived from host range assays and is measured as plaque forming unit (PFU) per mL. (PSA = *Pseudoalteromonas*, CBA = *Cellulophaga baltica*).

S2 Fig. Contact scores for each phage in SynCom-1 replicate. Black dots represent correct linkages and gray dots represent incorrect linkages.

S3 Fig. Receiver-operating characteristic (ROC) curve for normalized contact score and Z-score.

S4 Fig. Freeze-thaw experiments. A. Cell recovery after freeze thaw cycle. Unpreserved samples indicated bacteria flash frozen without any preservatives. **B.** Free DNA in frozen samples compared to fresh culture. The proportion of DNA in each pellet after freeze-thaw with various preservatives that is free, compared to culture.

S5 Fig. Number of Hi-C linkages in the peat samples. 'Different Contig Pairs' indicate all the raw chimeric reads that mapped to different viruses and/or hosts. 'Same Contig Pairs' refers to reads that map to same pair of contigs. 'Virus Host Pairs' indicate the subset of 'Different Contig Pairs' where each pair contains a read aligned to a virus and a host sequence.

S6 Fig. Host predictions (categorized at the phyla level) from Hi-C for peat samples. In each plot, the top bar shows viruses with any Hi-C linkage while the bottom bar includes only those with a Z-score ≥ 0.5. When multiple linkages were detected for a single virus, only the linkage with the highest normalized score was selected. Each phylum is represented by a different color, and the x-axis indicates the number of unique viruses.

S7 Fig. Comparison of host predictions (categorized at the phylum level) from Hi-C and iPHoP. The color represents whether the phylum-level host prediction was congruent or non-congruent between the two tools. The left panel shows all phylum predictions that occurred at least five times in the dataset. The right panel shows the same, but only includes Hi-C predictions with Z score ≥ 0.5.

S8 Fig. Breakdown of virus-host predictions from Hi-C and iPHoP, by congruency and Hi-C Z-score across taxonomic levels. The figure summarizes the agreement between virus-host predictions from Hi-C and iPHoP across multiple taxonomic ranks (e.g. domain, phylum, class). The black bars indicate predictions that were congruent from both tools and the grey bars indicate non-congruent predictions. Solid bars and striped bars indicate predictions where the Hi-C linkage had a Z-score of 0.5 and above, and below 0.5, respectively.

S1 Table. Synthetic community composition and concentrations. This table contains the full strain names (and abbreviated names) for each member of the synthetic community. Concentrations are listed in colony forming units (CFU) per mL for hosts or plaque forming units (PFU) per mL for phages. MOI was determined based on PFU/mL on the host of isolation (not necessarily the respective host in the community). The * denotes phages that do not infect any members of the mock community. The # denotes the currently available genome version with an update to follow.

S2 Table. Phage–host adsorption results. This table shows which phages adsorbed to which bacterial strains. Bacteria were grown to mid-exponential phase and incubated with phages at a multiplicity of infection (MOI) of 1. Bolded numbers show significant decrease in free phage over time (t-test).

S3 Table. Adsorption kinetics experiment after 15 minutes. The average percentage of starting phage adsorbed after 15 min is given, with standard deviation (SD), for each phage–host pair that showed significant adsorption based on the count of free phages present in the aliquot.

S4 Table. Information on sequenced samples. Numbers shown for raw Illumina and quality-cleaned reads. Numbers show reflect the numbers of paired reads.

S5 Table. Number of aligned pairs for each sample, categorized by alignment type. “Total Reads Aligned” are the number of pairs that aligned to the reference genome, “Different Contig Pairs” are read pairs in which each read aligned to a different genome, “Same Contig Pairs” are the read pairs that aligned to only one genome, “Poor Match Pairs” are the read pairs that had a poor match quality in the alignment, and “Single Reads” are read pairs where only one read of the pair aligned to any genome.

S6 Table. Contact and Z-scores for SynComs Hi-C linkages.

S7 Table. Sensitivity and Specificity of the synthetic communities before and after applying a threshold.

S8 Table. List of publications that used Hi-C to identify virus-host interactions.

S9 Table. Contact and Z-scores for peat Hi-C linkages

S10 Table. iPHoP predictions for Stordalen Mire vOTUs

S11 Table. VirMatcher predictions for Stordalen Mire vOTUs

S12 Table. Comparison of Hi-C and iPHoP predictions

S13 Table. Comparison of Hi-C and VirMatcher predictions

S14 Table. Hydrothermal Vent Linkages with Z-Score. The Z-score was calculated based on MAX_linkage for each rep_vMAG.

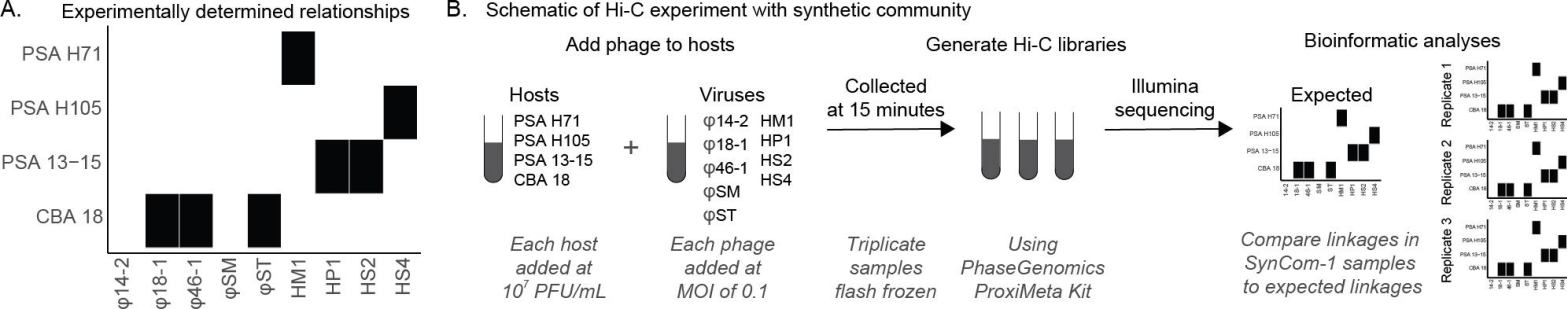
A.
Experimentally determined relationships
PSA H71
PSA H105
PSA 13−15
CBA 18
φ14-2
φ18-1
φ46-1
φSM
φST
HM1
HP1
HS2
HS4
B.
Schematic of Hi-C experiment with synthetic community
Add phage to hosts
Hosts
PSA H71
PSA H105
PSA 13-15
CBA 18
+
Viruses
φ14-2
φ18-1
φ46-1
φSM
φST
HM1
HP1
HS2
HS4
Each host added at 10^7 PFU/mL
Each phage added at MOI of 0.1
Generate Hi-C libraries
Collected at 15 minutes
Triplicate samples flash frozen
Illumina sequencing
Using PhaseGenomics ProxiMeta Kit
Bioinformatic analyses
Expected
Compare linkages in SynCom-1 samples to expected linkages
Replicate 1
Replicate 2
Replicate 3

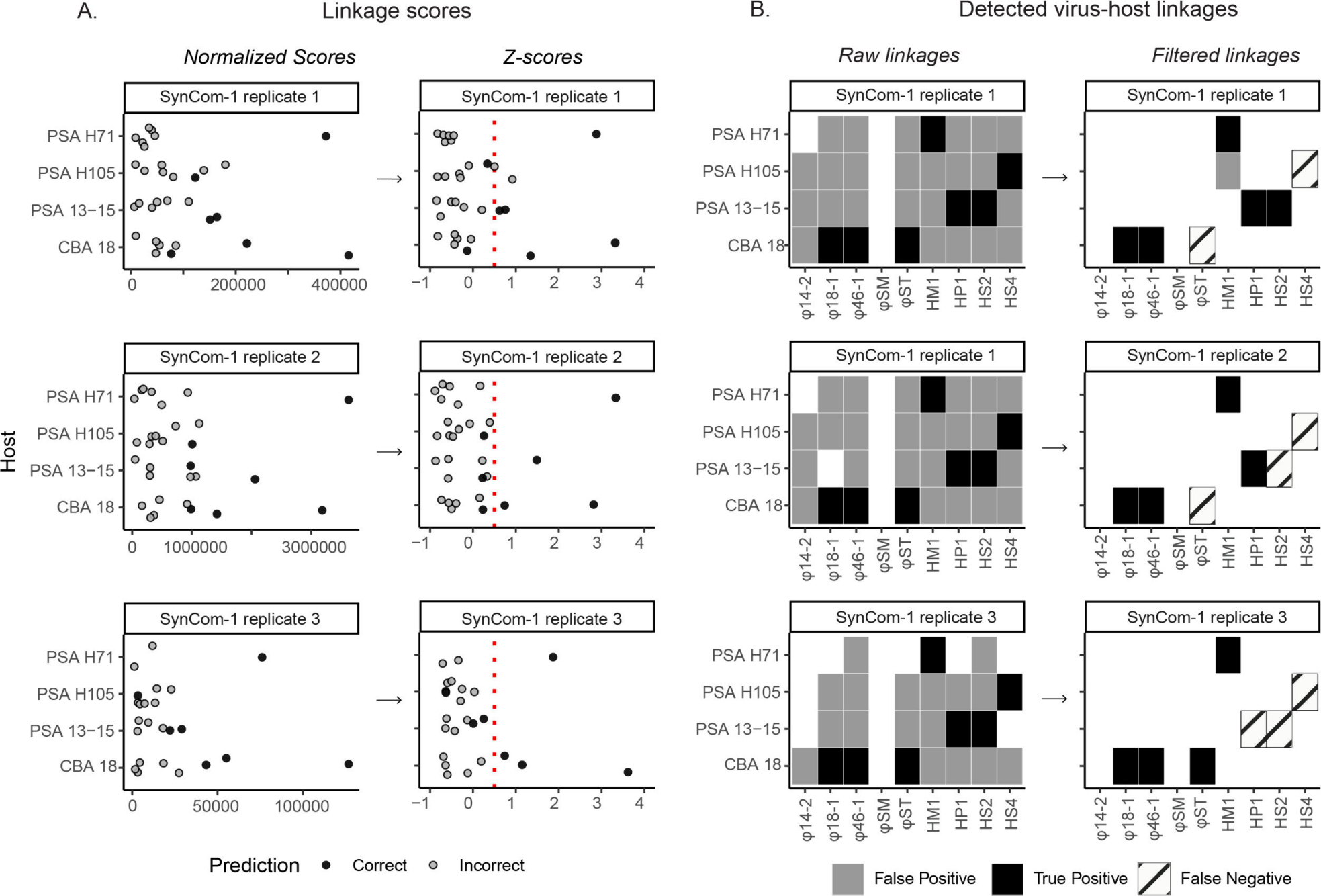
A.
Linkage scores
Normalized Scores
Z-scores
B.
Detected virus-host linkages
Raw linkages
Filtered linkages
SynCom-1 replicate 1
SynCom-1 replicate 2
SynCom-1 replicate 3
Host
PSA H71
PSA H105
PSA 13−15
CBA 18
0
200000
400000
1000000
3000000
50000
100000
−1
0
1
2
3
4
φ14-2
φ18-1
φ46-1
φSM
φST
HM1
HP1
HS2
HS4
Prediction
Correct
Incorrect
False Positive
True Positive
False Negative

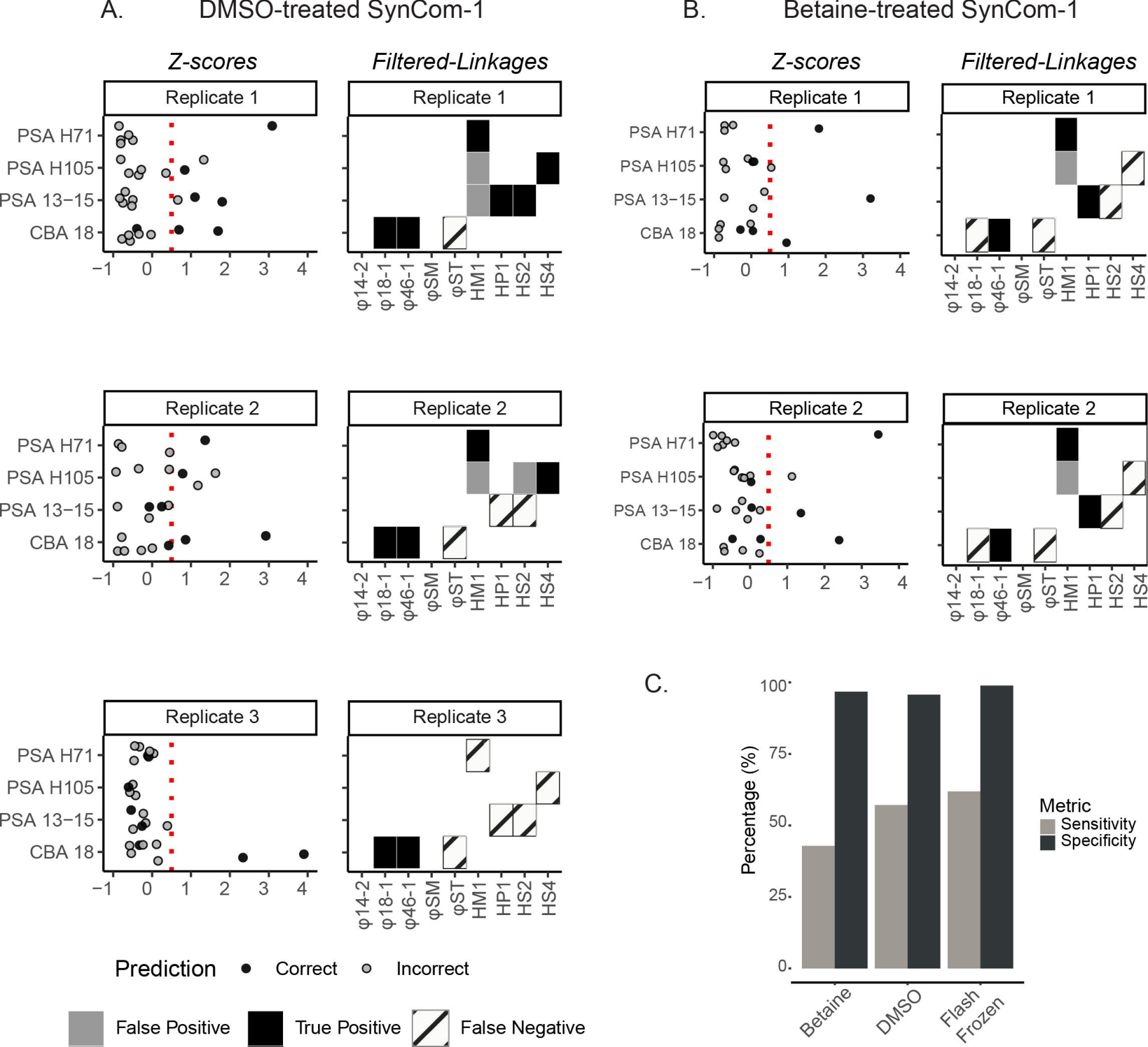
A.
DMSO-treated SynCom-1
B.
Betaine-treated SynCom-1
Z-scores
Filtered-Linkages
Replicate 1
Replicate 2
Replicate 3
PSA H71
PSA H105
PSA 13−15
CBA 18
−1
0
1
2
3
4
φ14-2
φ18-1
φ46-1
φSM
φST
HM1
HP1
HS2
HS4
Prediction
Correct
Incorrect
False Positive
True Positive
False Negative
C.
Percentage (%)
100
75
50
25
0
Metric
Sensitivity
Specificity
Betaine
DMSO
Flash Frozen

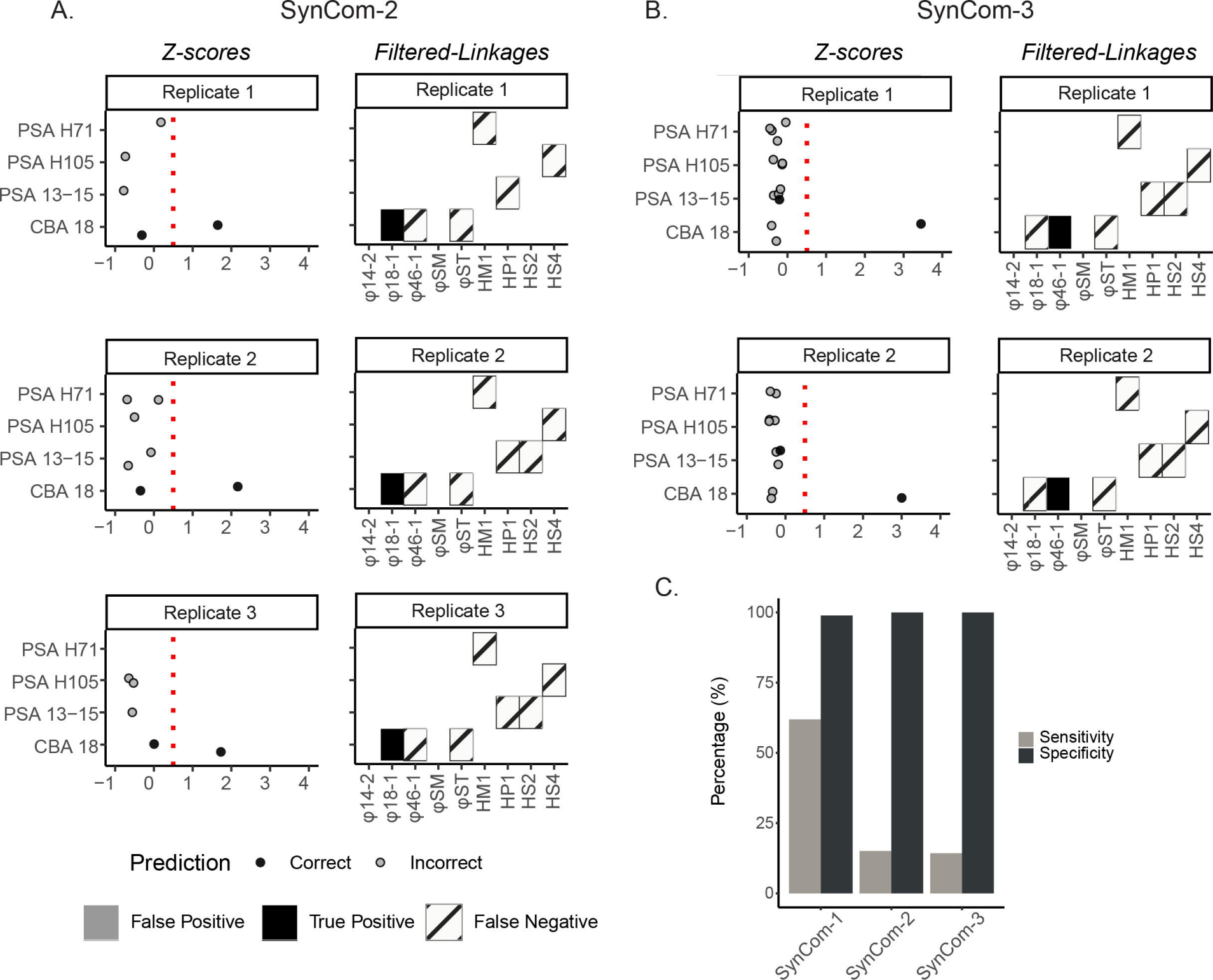
A.
SynCom-2
Z-scores
Filtered-Linkages
Replicate 1
Replicate 2
Replicate 3
PSA H71
PSA H105
PSA 13−15
CBA 18
−1
0
1
2
3
4
φ14-2
φ18-1
φ46-1
φSM
φST
HM1
HP1
HS2
HS4
Prediction
Correct
Incorrect
False Positive
True Positive
False Negative
B.
SynCom-3
C.
Percentage (%)
100
75
50
25
0
Sensitivity
Specificity
SynCom-1
SynCom-2
SynCom-3

A.

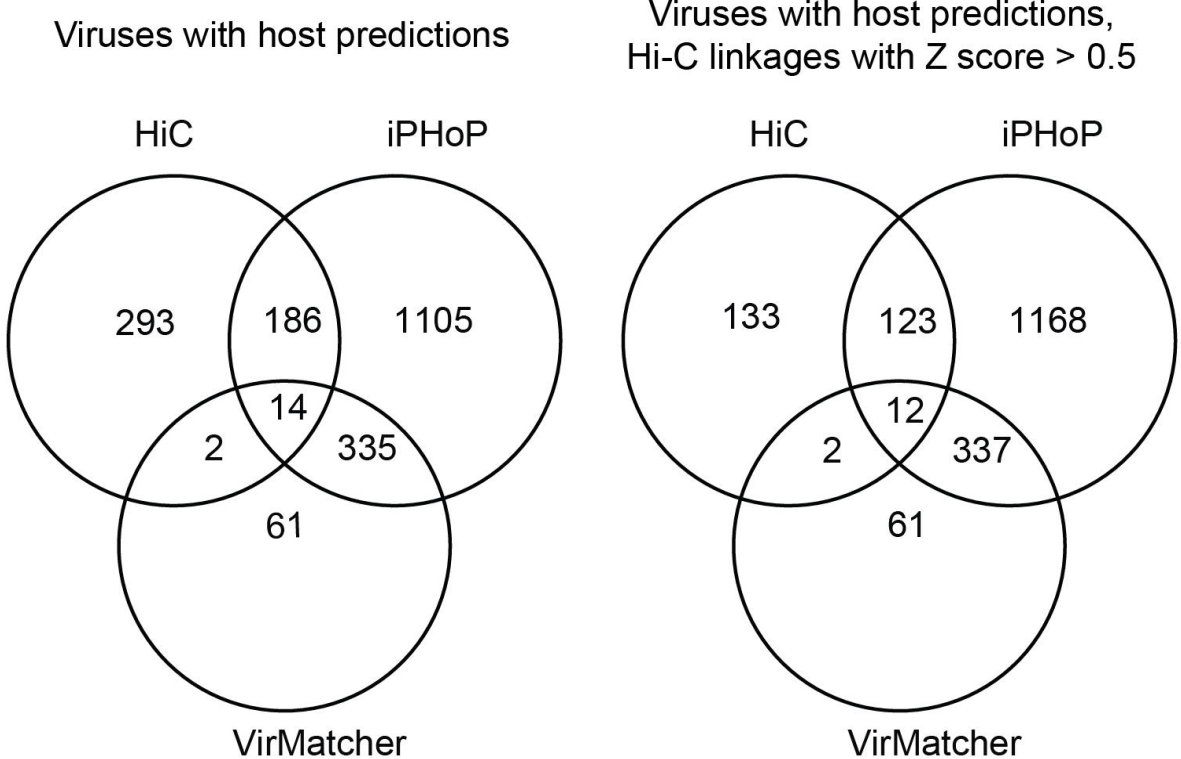
Viruses with host predictions
HiC
iPHoP
293
186
1105
14
2
335
61
VirMatcher
Viruses with host predictions,
Hi-C linkages with Z score > 0.5
HiC
iPHoP
133
123
1168
12
2
337
61
VirMatcher

B.

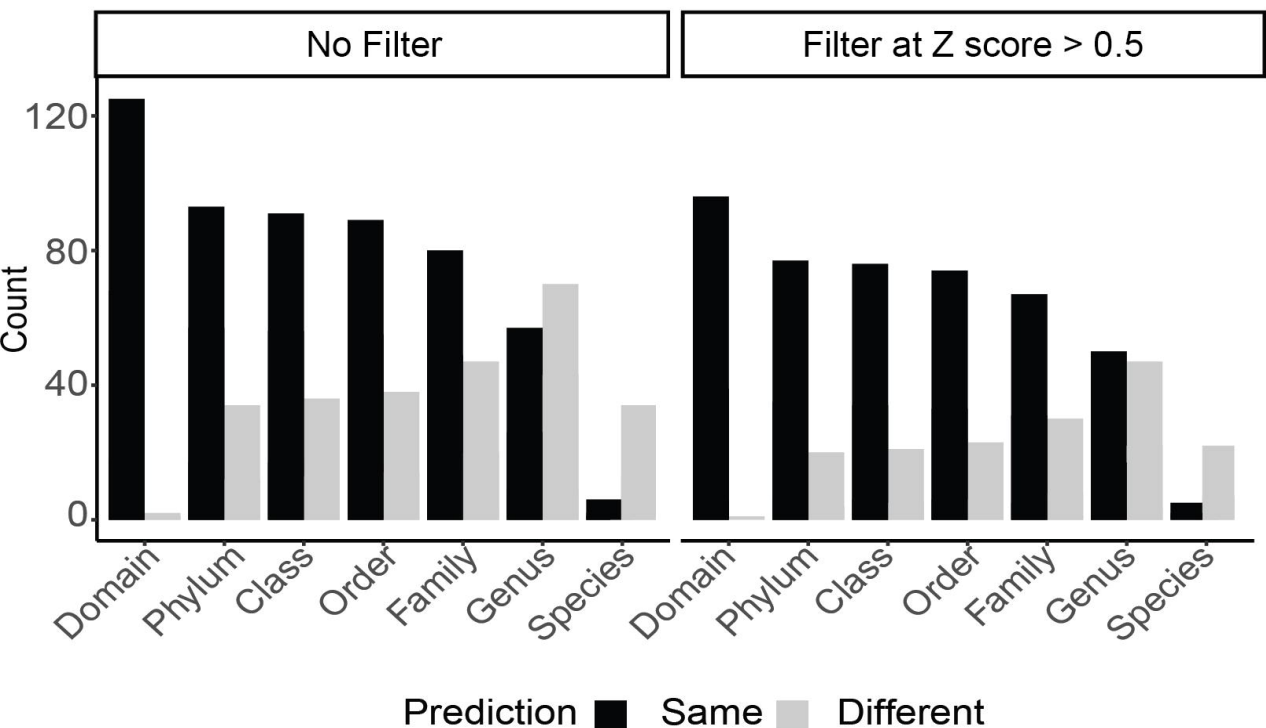
No Filter
Filter at Z score > 0.5
Count
120
80
40
0
Domain
Phylum
Class
Order
Family
Genus
Species
Prediction
Same
Different